ELSEVIER

#### Contents lists available at ScienceDirect

### Polymer

journal homepage: www.elsevier.com/locate/polymer



# Single electrospun PLLA and PCL polymer nanofibers: Increased molecular orientation with decreased fiber diameter



Jinglin Liu <sup>a</sup>, David Y. Lin <sup>b</sup>, Bin Wei <sup>a</sup>, David C. Martin <sup>a,\*</sup>

- <sup>a</sup> Department of Materials Science and Engineering, The University of Delaware, Newark, DE, 19716, United States
- <sup>b</sup> Strato, Inc., New York, NY, United States

#### ARTICLE INFO

Article history: Received 13 December 2016 Received in revised form 10 April 2017 Accepted 26 April 2017 Available online 27 April 2017

Keywords: Electrospinning Nanofiber Molecular orientation Electron microscopy

#### ABSTRACT

Electrospinning has become a widely-used method for fabricating polymer nanofibers for various applications including filtration, drug delivery, and tissue engineering. Due to the high extensional forces during the electrospinning process, and the rapid crystallization and solidification during solvent evaporation, molecular orientation may develop within the resulting fibers. The properties of electrospun fibers are expected to be sensitive to level of orientation in the fibers. Various reports have shown an increased modulus with decreased fiber diameter, and molecular orientation has been used to explain this trend. However, there have been relatively few studies of the detailed relationship between fiber diameter and molecular orientation, especially at the single fiber level. Here we report a quantitative study of the orientation in individual electrospun poly(caprolactone) (PCL) and poly(L-lactic acid) (PLLA) fibers using low-dose electron microscopy and diffraction techniques. Our results confirmed that for electrospun fibers of PCL and PLLA processed under similar experimental conditions, the molecular orientation decreased as the fiber diameter increased. The extent of orientation remained high for quite large fiber diameters, with azimuthal orientation of 20° seen up to ~500 nm for PCL and ~2000 nm for PLLA.

© 2017 Elsevier Ltd. All rights reserved.

#### 1. Introduction

Electrospinning has generated intense recent interest because of its ability to fabricate polymer fibers with nominal diameters  $(\sim 3 \text{ nm} - 1 \mu\text{m})$  about two to three orders of magnitude smaller than fibers manufactured via typical drawing, melt spinning, dry and wet jet spinning methods (10  $\mu$ m $-100 \mu$ m) [1,2]. In the common electrospinning process, electrostatic forces are used to distort a pendant droplet of polymer solution into a fine filament onto a conducting substrate. A wide variety of polymer fibers including polyethylene, polystyrene, polylactides, poly(vinylidene fluoride), and polyamides have been generated by electrospinning over the years [3]. The ability of this process to produce extremely fine fibers, as well as a number of interesting fiber morphologies has made it an attractive area of research for a number of different applications including protective clothing systems, separation membranes [4], and tissue scaffolds [5,6]. Modified collectors including rotating disks or gapped substrates have been employed

to prepare macroscopically aligned electrospun fibers for specific uses including directed neural regeneration [7–9].

The strong elongation forces and rapid solidification during the electrospinning process leads to distinct crystallization behavior in electrospun fibers when compared with polymers in larger fibers. Considerable effort has been invested in analyzing the structure and properties of electrospun fibers [10], but a number of important questions remain. Recent studies of the thermal and mechanical properties of single electrospun fibers showed a close relationship between fiber diameter and their thermal and mechanical properties. Several studies have shown increased mechanical properties with decreased fiber diameter [11–13]. Tan et al. [11] confirmed the significantly increased Young's modulus for electrospun poly(1-lactic acid) (PLLA) fibers with decreased diameters. Shin et al. [12] and Dzenis et al. [13] confirmed the same trend for poly(2-acrylamido-2-methyl-1-propanesulfonic acid) and polyacrylonitrile electrospun fibers.

The intrinsic orientational order developed during electrospinning is expected to be a key factor determining the properties of electrospun fibers, and has been suspected as a primary reason for the fiber diameter dependent thermal and mechanical

<sup>\*</sup> Corresponding author.

E-mail address: milty@udel.edu (D.C. Martin).

properties [10]. Various molecular orientation studies at the electrospun fiber mat level have revealed preferred orientation between the polymer backbone and the nanofiber axis. However, these results are usually not able to determine the orientation within single filaments, due to complexities from the unavoidable relative misalignment of electrospun fibers within a given bundle.

Molecular orientation studies of electrospun fibers at the single fiber level using advanced characterization techniques have been a promising means for targeting this problem. Selected area electron diffraction (ED) is a powerful tool for resolving orientation at the single fiber level. Huang et al. [14] confirmed a high level of molecular orientation in random nylon-4,6 electrospun fibers. Yoshioka et al. [15] did a systematic study confirming that smaller fibers showed higher level of molecular orientation for electrospun polyethylene (PE) fibers on aluminum foil collectors. Ma et al. [16,17] further investigated the effect of a gapped collector on the molecular orientation of electrospun PVDF fibers. They concluded that aligned fibers in air gap showed a much higher level of molecular orientation than fibers deposited in random mats, and the molecular orientation level increased with larger gap width. Reneker et al. [18,19] reported the molecular imaging of single electrospun PVDF fibers and confirmed the same molecular orientation that polymer chains were parallel to fiber axis, and further atomic scale features of PVDF in electrospun nanofibers were explored via high-resolution imaging by aberration corrected transmission electron microscopy. Gong et al. [20] investigated the influence of collecting method on the polymorphism and molecular orientation within electrospun poly[(R)-3-hydroxybutyrate-co-(R)-3-hydroxyhexanoatel (PHBHx) nanofibers using both electron diffraction and nanoscale AFM-IR techniques, and reported the strain-induced metastable β-form crystal structure and enhanced molecular orientation within macroscopically aligned fibers from modified collectors. Pellerin et al. [21] recently studied the orientation and partial disentanglement in individual electrospun atactic polystyrene (PS) fibers using polarized Raman spectroscopy. Despite these few studies on the single fiber molecular orientation, there is still a large deficiency in the understanding of the dependence between molecular orientation levels with fiber diameter for various electrospinning systems.

Aliphatic polyesters like PLLA and PCL have received considerable interest as one of the most promising biodegradable polymers. Their mechanical properties, thermoplastic processability, biodegradability and biocompatibility within the human body have made them attractive materials for a number of different applications [22–25]. However, despite the wide interest and confirmed increase in mechanical properties with decreased fiber diameters for these materials, no experimental data has yet confirmed the hypothesis that increased molecular orientation exists with decreased fiber diameters. The limited amount of systematic molecular orientation studies of PLLA and PCL electrospun fibers at single fiber level is presumably due to experimental difficulties. Both PLLA and PCL are extremely sensitive to the electron beam, requiring careful use of low dose techniques to extract information about the orientation of single filaments [26]. Specifically, the beam sensitivity of PLLA, as estimated by the critical dose required to cause fading of the predominant equatorial Bragg reflections corresponding to lateral packing distances between chains, has been estimated as 0.0002–0.0006 C/cm<sup>2</sup> or about 20–50 times smaller than polyethylene used in Yoshioka's study [15]. We have established that the beam sensitivity of PCL is about 0.002 C/cm<sup>2</sup>, which is still about 5 times more sensitive than polyethylene. Here we quantitatively examine the relationship between the fiber diameter and the local degree of molecular orientation in single electrospun PLLA and PCL filaments using low dose electron microscopy and diffraction techniques.

#### 2. Materials and methonds

#### 2.1. Materials

Poly(L-lactide) (PLLA) was purchased from Boehringer Ingelheim GmbH & Co. KG Fine Chemicals under the trade name Resomer® L210 (inherent viscosity: 3.3–4.3 dl/g, corresponding to an estimated molecular weight of 240,000–320,000 from the Mark-Houwink relationship). Poly(caprolactone) (PCL) (estimated molecular weight of 70,000–90,000) and 2,2,2-trifluoroethanol were purchased from Sigma-Aldrich. All chemicals were used as received unless otherwise specified.

#### 2.2. Electrospinning

PLLA powders were stirred in chloroform at 50–60 °C for 3–8 h to make a 3.0 wt % polymer solution suitable for electrospinning. The polymer solution was drawn into a 3 ml plastic syringe from Becton-Dickinson, and Co. and a #15 GP (1.37 mm diameter) needle tip from EFD, Inc. was attached to the syringe. The polymer solution supply rate was controlled at 0.15–0.75 ml/h using a syringe pump model KDS 100 from KD Scientific. The electrospinning voltage was +8.0 kV generated by a Hipotronics R10B HV DC power supply and the distance from the tip of the syringe to the edge of the spinning wheel was 7 cm. One end of the electrode from the power supply was attached to the needle tip, while the other end was connected to a spinning aluminum wheel. PLLA fibers were electrospun onto rectangular pieces of carbon-coated mica sheets that were mounted at the edge of the wheel. The wheel was spinning at 650 rpm, which is approximately 8.67 m/sec in linear speed, during electrospinning. After electrospinning, the samples were floated off onto deionized water and collected onto copper grids. Then, 10 nm of gold was sputtered coated onto the samples to improve contrast and provide an internal calibration standard for transmission electron microscopy (TEM) analysis. These samples were then annealed at 130 °C for 20 h to improve their crystallinity before further investigation.

PCL was stirred in 2,2,2-trifluoroethanol at room temperature overnight to make an 8.0 wt% polymer solution for electrospinning. The solution was drawn into a 3 mL syringe with a 14 gauge needle. The polymer solution supply rate was controlled at 0.5 mL/h with a syringe pump, and the working distance was set to 15 cm. An electrospinning voltage of  $+8.0~\rm kV$  on the needle tip and  $-4~\rm kV$  on the collector was applied, and modified collector with air gap (40 mm  $\times$  10 mm) was used to collect the resulting aligned PCL fibers

#### 2.3. Characterization

Wide-angle x-ray scattering (WAXS) patterns were obtained using a Rigaku Geigerflex 2D X-ray diffraction facility with Ni-filtered Cu K $\alpha$  radiation ( $\lambda=0.154$  nm) with pinhole collimation and a 2-D wire-detector. Well-aligned PLLA fiber bundles were mounted at the exit of the collimator and WAXS patterns were generated at 40 kV and 20 mA.

TEM and ED analysis of PLLA fibers were conducted using a Philips CM12 Analytical Electron Microscope. Low dose TEM techniques were employed because of the high electron beam sensitivity of PLLA electrospun fibers. Bright field (BF) images and electron diffraction patterns were captured under conditions well below the measured Total End Point Dose (TEPD) of 0.0002–0.0006 C/cm² (estimated at 300 kV using a JEOL 3011 High Resolution Electron Microscope). In this study, searching for sections of the sample suitable for imaging was typically done using a spot size of 11 under Diffraction Mode. When a section of interest

was found, it was translated a small amount away from the beam and conditions appropriate for imaging were set. The sample was then translated back and the photos and diffraction patterns were acquired.

For electrospun PCL fibers, both bright field (BF) images and ED patterns were acquired with a JEOL JEM-2010F FasTEM with 200 kV accelerating voltage. The TEPD of electrospun PCL fibers was estimated at ~0.002 C/cm². Digital images were analyzed with ImageJ (National Institute of Health) software.

#### 3. Results and discussion

## 3.1. Molecular orientation within aligned electrospun PLLA fiber bundles

Various reports have examined the crystallization and orientation within electrospun PLLA fibers and conclusions differed depending on the specific system for preparing the fibers [27–32]. Generally, less volatile solvents like chloroform [28] allowed the polymer jets to be stretched and extended more significantly before deposition than more volatile solvents like dichloromethane [33]. Therefore, the fibers electrospun from chloroform were more likely to experience significant shear and developed higher orientational order during electrospinning. In addition, aligned fibers collected on a rotating wheel [27] experienced further elongation and shearing and tended to develop higher orientational order.

In this study, the molecular orientational order that developed in electrospun PLLA fibers during electrospinning was first explored at fiber bundle level from Wide-angle X-ray Scattering (WAXS) (Fig. 1). As shown in Fig. 1a, the as-received PLLA powder displayed a nearly homogeneous azimuthal intensity distribution, indicating a lack of orientational order on a local scale. The more intense ring had a d-spacing of 0.52 nm, which corresponded to (110) d-spacing. The less intense ring had a d-spacing of 0.45 nm, which corresponded to the (111) d-spacing. After electrospinning, the aligned PLLA fibers began to show some orientational order as shown in Fig. 1b. The equatorial arcs of the more intense 0.52 nm (110) ring exhibited a significantly higher intensity than the meridional arcs. The fiber orientation was seen even more clearly after annealing the aligned, electrospun PLLA fibers. In addition to the 0.52 nm (110) reflection, reflections on the second (102) and third (103) layer lines with d-spacings of 0.40 and 0.29 nm were also observed. Another reflection that was observed was the set of arcs with a spacing of 0.46 nm (111), next to the (110) arc in the equatorial direction.

The WAXS results confirmed the existence of molecular orientation within the electrospun PLLA fibers, with a clearer trend observed for fibers after annealing. But these reflections were spread out largely due to the misalignment of different fibers in the fiber bundle. Because of the relatively large cross-section of the collimated beam (~300  $\mu m$ ), WAXS could not provide more detailed information about degree of the actual orientational order within the individual nanofibers.

#### 3.2. Molecular orientation within single electrospun PLLA fibers

To further investigate the molecular orientation within electrospun fibers, electron diffraction of single electrospun PLLA fibers was performed to eliminate the influence of misalignment between different fibers in the bundles needed to obtain WAXS results. To successfully acquire electron diffraction patterns of PLLA fibers with TEM, low dose techniques were used to minimize the exposure of the sample to the electron beam in order to preserve the features for analysis due to the high electron beam sensitivity of PLLA.

Electron diffraction patterns of individual electrospun PLLA fibers are shown in Fig. 2. Electron diffraction patterns of the electrospun PLLA fibers showed much narrower and sharper reflections than WAXS. By comparing the ED patterns and BF field images of individual fibers, it was confirmed that polymer chains were oriented parallel to fiber axis. We also found that the orientation of the chains were systematically higher in fibers with smaller diameters. As an example, Fig. 2c shows a diffraction pattern with two PLLA fibers that were about 45° imaged at the same time. The smaller fiber (350 nm in diameter) produced a sharper reflection ( $\alpha = 10.5^{\circ}$ ) compared to the larger one (1000 nm in diameter) which had a reflection angle  $\alpha$  of 14.2°.

As the diameter of the nanofibers increased, the resulting ED patterns systematically changed from sharp spots to diffuse arcs as shown in Fig. 3. Electron diffraction patterns of various single electrospun PLLA fibers with a wide range of different diameters were taken and compared with their fiber diameter. To quantify the degree of orientation, the azimuthal angle  $(\alpha)$  of the equatorial (110) diffraction peak was determined from the ED pattern, using the full width at half maximum intensity. A smaller value of  $\alpha$  means a higher degree of molecular orientation within the fiber. The experiments results were compiled for more than 16 different fibers and are plotted in Fig. 4a. It is evident that as the fiber diameter decreased, the tangential spread decreased significantly, leading to systematically increased molecular orientation of the crystalline regions.

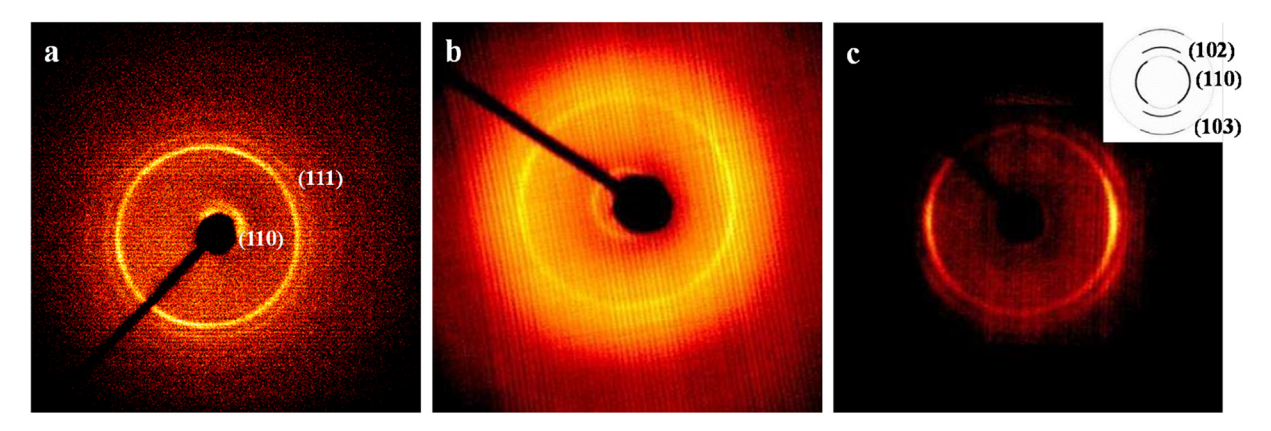


**Fig. 1.** WAXS data of: (a) PLLA powder as-received showing homogeneous azimuthal intensity distribution of (110) and (111); (b) electrospun PLLA fibers aligned by the spinning wheel substrate showing more intense equatorial arcs of the 0.52 nm (110) ring than the meridional arcs; and (c) after annealing the electrospun fibers at 100 °C for 10 min showing clearer orientational order.

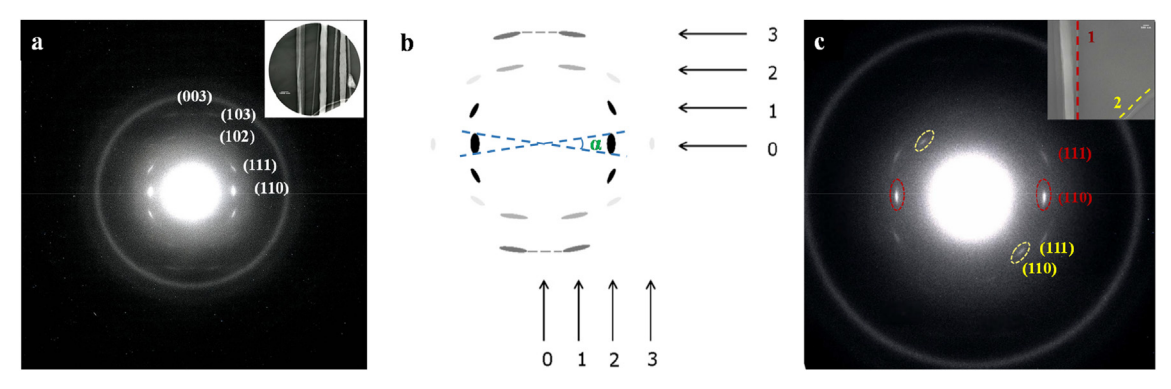


**Fig. 2.** (a) Electron diffraction pattern of well aligned electrospun PLLA fibers with fiber diameters ranging from 150 to 1000 nm; (b) schematic drawing of this ED pattern showing the azimuthal angle  $\alpha$ ; (c) two sets of ED fiber patterns from two distinctly oriented electrospun PLLA fibers (labeled as 1, 2). The smaller fiber shows a higher degree of orientation (350 nm. 10.5°) than the larger one (1000 nm diameter, 14.2°).

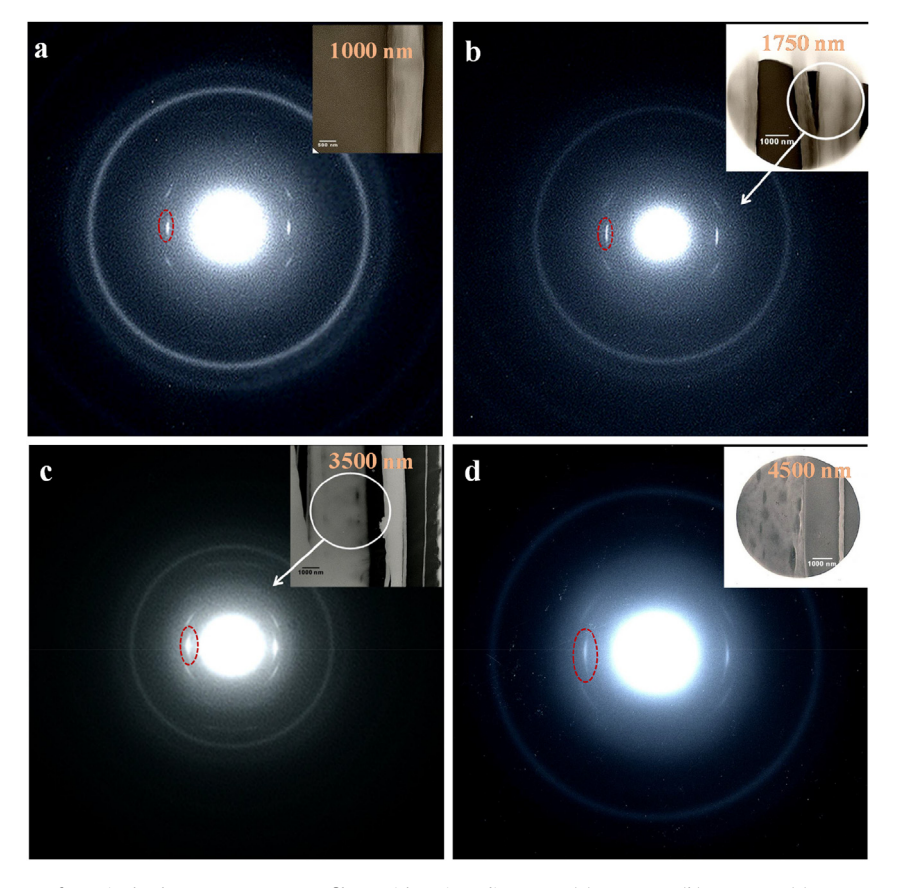


Fig. 3. ED fiber patterns from single electrospun PLLA nanofibers with various diameters: (a) 1000 nm; (b) 1750 nm; (c) 3500 nm; and (d) 4500 nm.

#### 3.3. Molecular orientation within single electrospun PCL fibers

We have analyzed the relationship between molecular orientation and fiber diameter for electrospun PLLA fibers aligned with a rotating wheel. As a comparison, we also prepared macroscopically aligned PCL fibers by introducing an air gap in the substrate and analyzed the ED patterns from individual aligned PCL fibers (Fig. 5). By comparing the ED pattern and the BF images, it was revealed that polymer chains were preferentially oriented parallel to fiber axis for the PCL fibers, similar to the orientation within PLLA fibers. Fig. 5 shows ED patterns from different individual electrospun PCL fibers. With increasing fiber diameters, the ED patterns changed to more diffuse arcs, again indicating a larger degree of polymer chain

misalignment. By quantitatively measuring the azimuthal angle ( $\alpha$ ) of the strongest equatorial arc-shaped (110) diffraction peak from the ED pattern, there was again a clear trend of increased molecular orientation for decreased fiber diameters. This trend of decreased molecular orientation with increased fiber diameter correlated well with the similar relationship determined for PLLA fibers (Fig. 4a).

#### 3.4. Molecular orientation within single electrospun fibers

We have confirmed that for both electrospun PLLA and PCL fibers, molecular orientation increased as fiber diameter decreased. When we plotted the azimuthal angle of the first strongest reflection from the ED pattern as a function of fiber diameter, the trends

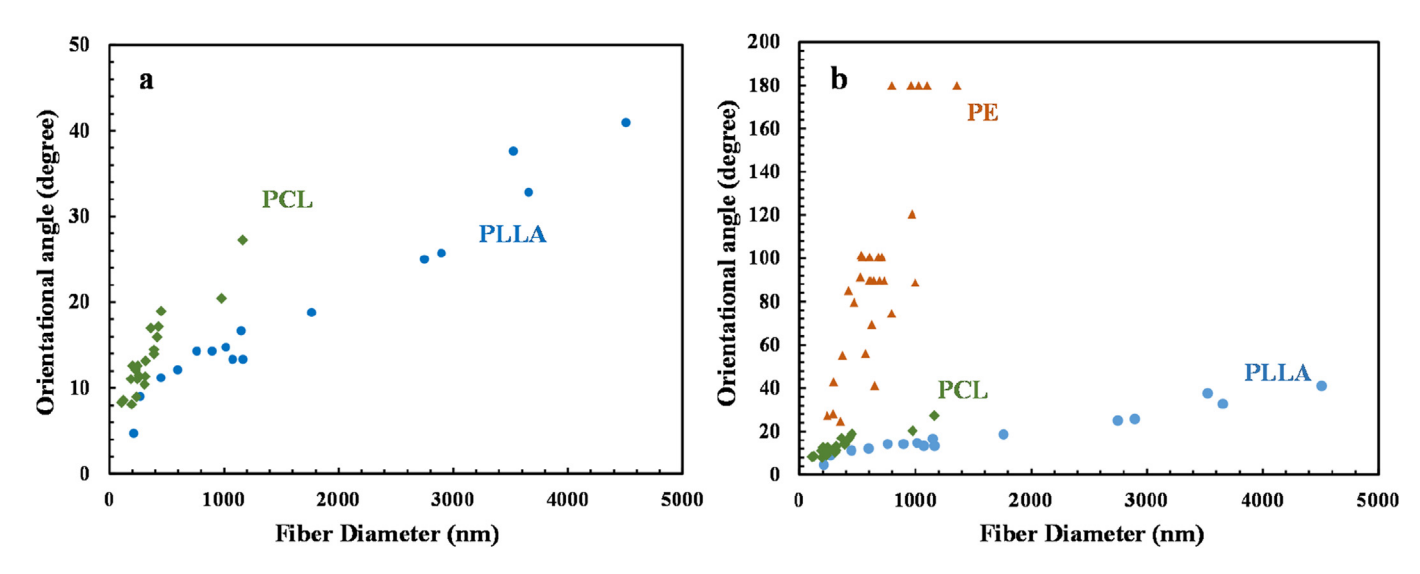


Fig. 4. Relationship between fiber diameter and degree of orientation for (a): aligned electrospun PLLA (circles) and PCL fibers (diamonds). The arc angle of the first strongest reflection from the ED pattern was plotted against fiber diameter. (b) Plot of aligned electrospun PLLA and PCL fibers, and electrospun PE fibers from Yoshioka (triangles) [15].

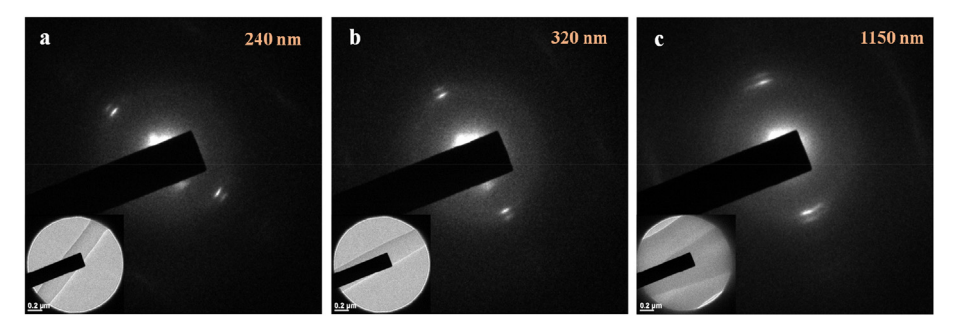


Fig. 5. ED fiber patterns from electrospun PCL fiber with widths of: (a) 240 nm; (b) 320 nm; (c) 1150 nm.

for both fibers were similar (Fig. 4a). The electrospun PLLA and PCL fibers maintained a relatively high orientation even at fairly large diameters, with an orientation of  $\sim\!20^\circ$  still seen at  $\sim\!2000$  nm for PLLA, and  $\sim\!500$  nm for PCL.

The overall trend of increased molecular orientation with decreased fiber diameters was similar to that seen in Yoshioka's previous investigation on electrospun PE fibers [15], but the degree of orientation was substantially different (Fig. 4b). For the PE fibers, a similar high degree of orientation was only observed for the smallest nanofibers (~200 nm), and the larger fibers (above ~1000 nm) were essentially randomly oriented. Possible reasons might be the difference in the chain flexibility and variations in the details of the electrospinning setup. PLLA and PCL chains are not as flexible as PE, and thus would not be able to relax as much as PE before solidification into the final fiber. In addition, room temperature electrospinning was used for the PLLA and PCL fibers studied in this report, whereas a high temperature solution was used for electrospinning PE in Yoshioka's study. Furthermore, a rotating wheel or air gap was used to macroscopically align the fibers. Both the difference in processing temperature and the fiber collecting method would be expected to result in extra stretching force for PCL and PLLA fibers, leading to better molecular orientation.

The trends of increased molecular orientation with decreased fiber diameter we have confirmed experimentally here correspond well with the previous reports showing significantly enhanced mechanical properties with decreased nanofiber diameter. Tan reported an enhanced Young's modulus for single electrospun PLLA

fibers with diameters smaller than 350 nm [11]. Dzenis reported the simultaneously enhanced modulus, strength and toughness of single electrospun polyacrylonitrile nanofibers with decreased fiber diameter, and the most dramatic increases were recorded for fibers with diameters less than 250 nm [13].

To estimate the length scales over which the effect of surface induced alignment was felt, we examined a simple confinement model of the orientation, assuming that the responding elements were rigid, linear entities. If the induced orientation was due only to the surface confinement of a rigid element of some length  ${\bf l}$  into a fiber with diameter of  ${\bf d}$  (Fig. 6a), the expected azimuthal orientation angle could be calculated as  $\alpha=2$  ArcSin[d/l]. An estimate of  ${\bf l}$  ( ${\bf l}=3200$  nm for PLLA and  ${\bf l}=1200$  nm for PCL) was acquired for both fibers from the plot. The model was a better fit for fibers with smaller diameters (less than 200–400 nm), where the mechanical properties were typically significantly higher [11,13].

The fact that the length scales **I** determined by this analysis (1000–3000 nm) are much larger than the molecular dimensions of individual chains (10–20 nm) indicates that the electrospinning is influencing the relative orientation of the polymers in the nanofiber over these relatively large dimensions. This simple surface confinement model does not fit as well at larger diameters (Fig. 6b), indicating that the actual process of molecular alignment was much more complicated than mere surface confinement, especially for these larger fibers. The strong elongation forces during the electrospinning and drawing processes would likely lead to a high degree of alignment for only a few chains, leaving the

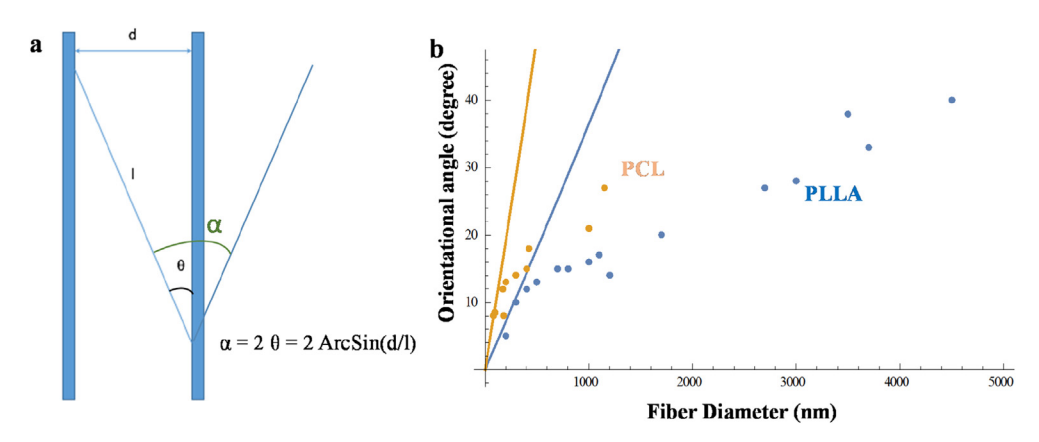


Fig. 6. (a): Model for confinement of rigid element of length 1 and fiber diameter d. (b): Estimate of 1 for both PLLA and PCL electrospun fibers.

rest of them fall into place as the fiber solidified during evaporation, similar to the shish-kebab model for polymers crystallizing from an oriented melt under shear.

Our experimental results provide insights about the relationship between local nanofiber orientation and diameter in two different polymer systems (PLLA and PCL). However there are many issues that are still unknown. The detailed relationship between processing variables, fiber diameter, and degree of orientation will require a systematic study of the alignment, extension, and solidification of the chains during solvent evaporation. Future studies would benefit from improvements in instrumentation that would allow for direct measurements on single nanofibers during solvent evaporation, perhaps using synchroton X-ray scattering or suitably modified in-situ stages that are now available for the TEM [34].

#### 4. Conclusions

Macroscopically aligned PLLA and PCL electrospun fibers were prepared with a rotating wheel and an air-gap modified collector. WAXS patterns confirmed the existence of an overall degree of molecular orientation within bundles of PLLA fibers. Low dose electron diffraction confirmed preferred molecular orientation at the single fiber level for both PLLA and PCL electrospun nanofibers. Using the intensity profile of the strongest reflection from the ED pattern, the orientational order of electrospun PLLA and PCL fibers was shown to be a function of fiber diameter. A clear trend of smaller arc angles (higher orientation) was confirmed for fibers with thinner diameters. Our results showed that for electrospun PLLA and PCL fibers, molecular orientation with single fiber increased with decreased fiber diameter. Possible mechanisms for the increased orientation during electrospinning and their correspondence with known trends of increased mechanical properties with decreased fiber diameters were discussed.

#### Acknowledgements

This research was supported in part by National Science Foundation (DMR-1103027 and DMR-1505144) and the University of Delaware.

#### References

- D. Li, Y. Xia, Electrospinning of nanofibers: reinventing the wheel? Adv. Mater 16 (2004) 1151–1170.
- [2] J. Doshi, D.H. Reneker, Electrospinning process and applications of electrospun fibers, Conf. Rec. 1993 IEEE Ind. Appl. Conf. Twenty-Eighth IAS Annu. Meet. 35 (1993) 151–160.
- [3] D.H. Reneker, A.L. Yarin, E. Zussman, H. Xu, Electrospinning of nanofibers from

- polymer solutions and melts, Adv. Appl. Mech. 41 (2007), 43-195.
- [4] P. Gibson, H. Schreuder-Gibson, D. Rivin, Transport properties of porous membranes based on electrospun nanofibers, Colloids Surfaces A Physicochem. Eng. Asp. 187–188 (2001) 469–481.
- [5] W.J. Li, C.T. Laurencin, E.J. Caterson, R.S. Tuan, F.K. Ko, Electrospun nanofibrous structure: a novel scaffold for tissue engineering, J. Biomed. Mater. Res. 60 (2002) 613–621.
- [6] J.A. Matthews, G.E. Wnek, D.G. Simpson, G.L. Bowlin, Electrospinning of collagen nanofibers, Biomacromolecules 3 (2002) 232–238.
- [7] M.V. Kakade, S. Givens, K. Gardner, K.H. Lee, D.B. Chase, J.F. Rabolt, Electric field induced orientation of polymer chains in macroscopically aligned electrospun polymer nanofibers, J. Am. Chem. Soc. 129 (2007) 2777–2782.
- [8] P.-C. Chang, B.-Y. Liu, C.-M. Liu, H.-H. Chou, M.-H. Ho, H.-C. Liu, D.-M. Wang, L.-T. Hou, Aligned electrospun nanofibers specify the direction of dorsal root ganglia neurite growth, J. Biomed. Mater. Res. A 81 (2007) 771–780.
- [9] J.M. Corey, D.Y. Lin, K.B. Mycek, Q. Chen, S. Samuel, E.L. Feldman, D.C. Martin, Aligned electrospun nanofibers specify the direction of dorsal root ganglia neurite growth, J. Biomed. Mater. Res. A 83A (2007) 636–645.
- [10] M. Richard-Lacroix, C. Pellerin, Molecular orientation in electrospun fibers: from mats to single fibers, Macromolecules 46 (2013) 9473–9493.
- [11] E.P.S. Tan, C.T. Lim, Physical properties of a single polymeric nanofiber, Appl. Phys. Lett. 84 (2004) 1603–1605.
- [12] M.K. Shin, S.I. Kim, S.J. Kim, S.K. Kim, H. Lee, G.M. Spinks, Size-dependent elastic modulus of single electroactive polymer nanofibers, Appl. Phys. Lett. 89 (2006) 2004–2007.
- [13] D. Papkov, Y. Zou, M.N. Andalib, A. Goponenko, S.Z.D. Cheng, Y.A. Dzenis, Simultaneously strong and tough ultra fine continuous nanofibers, ACS Nano 7 (2013) 3324–3331.
- [14] C. Huang, S. Chen, C. Lai, D.H. Reneker, H. Qiu, Y. Ye, H. Hou, Electrospun polymer nanofibres with small diameters, Nanotechnology 17 (2006) 1558.
- [15] T. Yoshioka, R. Dersch, M. Tsuji, A.K. Schaper, Orientation analysis of individual electrospun PE nanofibers by transmission electron microscopy, Polymer 51 (2010) 2383–2389.
- [16] X. Ma, J. Liu, C. Ni, D.C. Martin, D.B. Chase, J.F. Rabolt, Molecular orientation in electrospun poly(vinylidene fluoride) fibers, ACS Macro Lett. 1 (2012)
- [17] X. Ma, J. Liu, C. Ni, D.C. Martin, D.B. Chase, J.F. Rabolt, The effect of collector gap width on the extent of molecular orientation in polymer nanofibers, J. Polym. Sci. Part B Polym. Phys. 54 (6) (2015) 617–623.
- [18] Z. Zhong, J.Y. Howe, D.H. Reneker, Molecular scale imaging and observation of electron beam-induced changes of polyvinylidene fluoride molecules in electrospun nanofibers, Polym. Guildf. 54 (2013) 3745–3756.
- [19] D. Lolla, J. Gorse, C. Kisielowski, J. Miao, P.L. Taylor, G.G. Chase, D.H. Reneker, Polyvinylidene fluoride molecules in nanofibers, imaged at atomic scale by aberration corrected electron microscopy, Nanoscale 8 (2016) 120–128.
- [20] L. Gong, D.B. Chase, I. Noda, J. Liu, D.C. Martin, C. Ni, J.F. Rabolt, Discovery of β-form crystal structure in electrospun poly[(R)-3-hydroxybutyrate-co-(R)-3-hydroxyhexanoate] (PHBHx) nanofibers: from fiber mats to single fibers, Macromolecules 48 (2015) 6197–6205.
- [21] M. Richard-Lacroix, C. Pellerin, Orientation and partial disentanglement in individual electrospun fibers: diameter dependence and correlation with mechanical properties, Macromolecules 48 (2015) 4511–4519.
- [22] L. Zhang, C. Xiong, X. Deng, Biodegradable polyester blends for biomedical application, J. Appl. Polym. Sci. 56 (1995) 103–112.
- [23] E.A.R. Duek, C.A.C. Zavaglia, W.D. Belangero, In vitro study of poly(lactic acid) pin degradation, Polym. Guildf. 40 (1999) 6465–6473.
- [24] Y. Ikada, H. Tsuji, Biodegradable polyesters for medical and ecological applications, Macromol. Rapid Commun. 21 (2000) 117–132.
- [25] R. Auras, B. Harte, S. Selke, An overview of polylactides as packaging materials, Macromol. Biosci. 4 (2004) 835–864.
- [26] D.C. Martin, J. Chen, J. Yang, L.F. Drummy, C. Kubel, High resolution electron

- microscopy of ordered polymers and organic molecular crystals: recent developments and future possibilities, J. Polym. Sci. Part B Polym. Phys. 43 (2005) 1749–1778.
- [27] X. Zhang, R. Nakagawa, K.H.K. Chan, M. Kotaki, Mechanical property enhancement of polylactide nanofibers through optimization of molecular weight, electrospinning conditions, and stereocomplexation, Macromolecules 45 (2012) 5494–5500.
- [28] H. Tsuji, M. Nakano, M. Hashimoto, K. Takashima, S. Katsura, A. Mizuno, Electrospinning of poly(lactic acid) stereocomplex nanofibers, Biomacromolecules 7 (2006) 3316–3320.
- [29] C. Ribeiro, V. Sencadas, C.M. Costa, I.L. Gómez Ribelles, S. Lanceros-Méndez. Tailoring the morphology and crystallinity of poly(L-lactide acid) electrospun membranes, Sci. Technol. Adv. Mater 12 (2011) 015001.
- [30] J. Ren, W. Liu, J. Zhu, S. Gu, Preparation and characterization of electrospun,

- biodegradable membranes, J. Appl. Phys. 109 (2008) 3390—3397. [31] A.M. El-Hadi, S.D. Mohan, F.J. Davis, G.R. Mitchell, Enhancing the crystallization and orientation of electrospinning poly (lactic acid) (PLLA) by combining with additives, J. Polym. Res. 21 (2014) 605.
- [32] J.E. Oliveira, L.H.C. Mattoso, W.J. Orts, E.S. Medeiros, Structural and morphological characterization of micro and nanofibers produced by electrospinning and solution blow spinning: a comparative study, Adv. Mater. Sci. Eng. (2013)
- [33] R. Dersch, T. Liu, A.K. Schaper, A. Greiner, J.H. Wendorff, Electrospun nanofibers: internal structure and intrinsic orientation, J. Polym. Sci. Part A Polym. Chem. 41 (2003) 545-553.
- [34] J. Liu, B. Wei, J.D. Sloppy, L. Ouyang, C. Ni, D.C. Martin, Direct imaging of the electrochemical deposition of poly(3,4-ethylene dioxythiophene) (PEDOT) by tranmission electron microscopy, ACS Macro Lett. 4 (9) (2015) 897–900.